



HAL
open science

Dynamic HAADF-STEM Observation of a Single-Atom Chain as the Transient State of Au Ultrathin Nanowire Breakdown

Lise-Marie Lacroix, Raul Arenal, G. Viau

► **To cite this version:**

Lise-Marie Lacroix, Raul Arenal, G. Viau. Dynamic HAADF-STEM Observation of a Single-Atom Chain as the Transient State of Au Ultrathin Nanowire Breakdown. *Journal of the American Chemical Society*, 2014, 136 (38), pp.13075-13077. hal-02023288

HAL Id: hal-02023288

<https://insa-toulouse.hal.science/hal-02023288v1>

Submitted on 2 Mar 2021

HAL is a multi-disciplinary open access archive for the deposit and dissemination of scientific research documents, whether they are published or not. The documents may come from teaching and research institutions in France or abroad, or from public or private research centers.

L'archive ouverte pluridisciplinaire **HAL**, est destinée au dépôt et à la diffusion de documents scientifiques de niveau recherche, publiés ou non, émanant des établissements d'enseignement et de recherche français ou étrangers, des laboratoires publics ou privés.

Dynamic HAADF STEM observation of single atom chain as transient state of Au ultrathin nanowire breakdown.

Lise-Marie Lacroix,^{†*} Raul Arenal,^{‡**} Guillaume Viau[†].

[†] LPCNO, Université de Toulouse, INSA, UPS, LPCNO (Laboratoire de Physique et Chimie des Nano-Objets), F-31077 Toulouse, France; CNRS; UMR 5215 ; LPCNO, F-31077 Toulouse, France

[‡] Laboratorio de Microscopias Avanzadas (LMA), Instituto de Nanociencia de Aragon (INA), U. Zaragoza, C/ Mariano Esquillor s/n, 50018 Zaragoza (Spain).

^{*} Fundacion ARAID, 50004 Zaragoza, Spain.

Supporting Information Placeholder

ABSTRACT: Ultrathin chemically grown Au nanowires undergo irremediable structural modification under external stimuli. Thanks to dynamic high-angle annular dark field imaging, electron beam induced damaging was followed, revealing the formation of linear gold atom chains as long as reactive clusters on the side, opening fascinating perspectives for both catalysis and electronic transport applications.

Metallic nanowires represent ideal objects for fundamental studies as long as potential applications in sensing,¹ catalysis and electronic contacts.^{2,3} Quantized conductance scaling with $2e^2/h$ was observed in atomic wires obtained by mechanical deformation of point contact,^{4,5,6} breaking junction,⁷ electrochemical approaches.⁸ Recently, ultrathin gold nanowires exhibiting a diameter of 1.7 nm and a micrometric length were synthesized by reduction of gold chloride salt in presence of oleylamine.^{9,10,11,12} These highly crystalline wires, grown along the $\langle 111 \rangle$ direction of the fcc structure, opens great perspective for electronic transport studies.^{13,14} Their small diameter leads to quantized phenomena while their extreme aspect ratio render physical contact by lithography feasible.^{14,15} However, thin metal nanowires are prone to fragment into chain of spheres at high temperature, as described by the Plateau-Rayleigh instability.^{16,17} The critical temperature at which this phenomenon occurs is strongly dependent on the wire surface energy and thus on the crystalline surface exposed and on the ligands adsorbed.¹⁸ Other perturbation such as electron beam can also induce such instability.¹⁹ Radiolysis, due to plasmon losses, and knock-on damage, resulting from high energy scattering, are the two most common types of primary damage that occur in irradiated samples,²⁰ depending on their electronic state.^{21,22} We report here for the first time a dynamic study of the Au wire breaking by HAADF-STEM. Sub atomic resolution obtained with the aberration corrected microscope combined with the high diffusion of Au enabled to follow the trajectory of individual atoms, evidencing the formation of atom chains prior to the breaking and free clusters aside.

1.7 nm ultrathin Au nanowires were obtained in liquid phase following previously reported synthesis (Figure 1a).²³ Briefly, a 10 mM HAuCl₄ solution was reduced by triisopropylsilane in presence of oleylamine at 40°C for 1h30. The reducing agent and surfactant excess was removed by purification prior to the deposition of Au wires on the carbon coated Cu grid. Electron-beam shower, during 20-25 min, was performed in-situ to prevent contamination during STEM experiments. HAADF-STEM study was performed with an aberration corrected microscope working at 80 - 300 kV. The aberration-free probe is taken to have a 25 mrad converge semi-angle, providing a resolution of ~ 1.3 Å (80 kV) and ~ 0.8 Å (300 kV). The inner and outer collection angles used in recording the HAADF images were 60 and 200 mrad, respectively. Low electron doses of 0.0145 e⁻ Å⁻² s⁻¹ (80 kV) and 1.1 e⁻ Å⁻² s⁻¹ (300 kV) were employed.

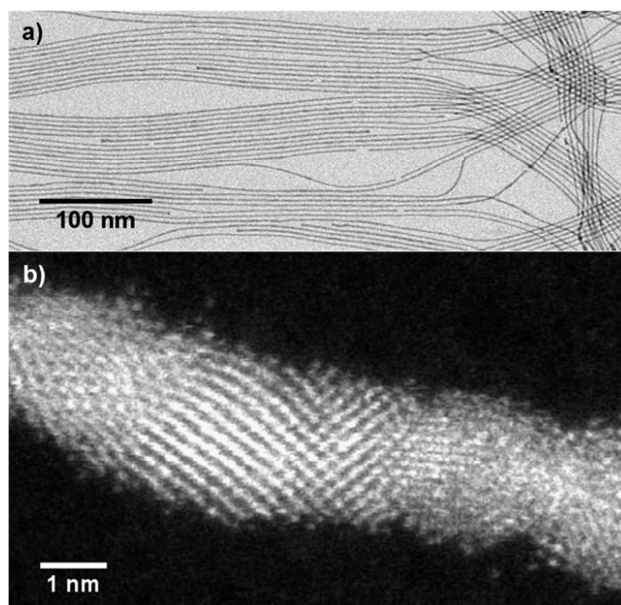


Figure 1. a) TEM and b) HAADF-STEM images of Au nanowires.

The Z-contrast nature of HAADF-STEM imaging makes this technique an ideal method for identifying heavy atoms (as gold, $Z=79$) on light supports (carbon, $Z=6$, in the present case) as evidenced in Figure 1b. Surprisingly, at 80 kV and under very low dose ($0.0145 \text{ e}^- \text{ \AA}^{-2} \text{ s}^{-1}$), the degradation of Au NWs was extremely fast (Video S1-S2). However, at 300 kV, the electron beam damaging could be dynamically followed using a 1.6 frame.s^{-1} scanning (Video S3-S9). It is well established that higher accelerating voltage reduces radiolysis damage due to lower inelastic scattering probability. However, opposite happens for knock-on damage, the threshold for gold clusters and particles being above 200 and 400 kV respectively.^{24,25} As a consequence, though gold is a good conductor, the evolution of these Au NW seems to be governed by radiolysis at low voltage.

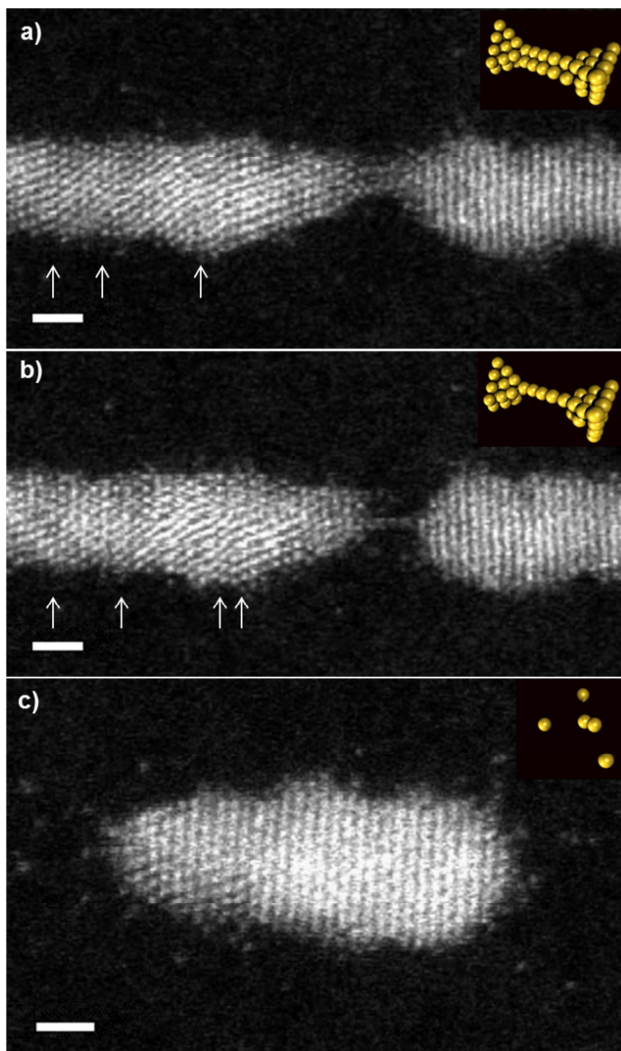


Figure 2. Snapshots extracted from video S3 of E-beam induced wire breaking which proceeds through the decrease of the channel diameter from a) 3 atoms to b) single atom. c) resulting 7 nm rods surrounded by Au atoms and dimers. As insets, schematic 3D views of a) MATC, b) SATC and c) dimer and isolated atoms. Scale bar : 1 nm. White arrows indicate twin planes

At 300 kV, atomic columns as long as individual atoms on the side of the wire could be detected as evidenced in Figure

1b. The wire breaking occurred through a continual structural reorganization, with multiple twin boundaries, as long as a thickening of the initial diameter, leading to rough surfaces, as evidenced in Figure 2 and supplementary videos S1.

Contrarily to the theoretical model of Plateau Rayleigh instability,²⁶ the breakdown involves first an asymmetric modification of the apexes. Moreover, prior to disruption, two types of chains were observed exhibiting 3-4 atoms (Video S3-S6 and Figure S1) or single-atom thickness (Video S3, S7-S8, Figure 2a-b and S2). The single-atom chains (SAC) results from the downsizing of the channel from 3-4 atoms down to a single one as evidenced by the successive snapshots in Figure 2a-b extracted from video S3. On the contrary, some multi-atom chains (MAC) exhibit a different behavior and break very suddenly (Figure S3). These two types were previously reported on gold nanowires obtained by HRTEM irradiation of a Au polycrystalline thin film.²⁷ Rodrigues et al. invoked the difference of crystalline orientation of the atom chains obtained, $[110]$ versus $[111]$ or $[100]$ respectively, to explain such discrepancy. Starting from single-crystalline Au nanowires grown along $\langle 111 \rangle$ direction, we did not expect such variety.

Due to the constant rotation of the wire under the electron beam, the atomic positions could not always be resolved. We followed two cases of single atom chain (SAC) and multi atom chain (MAC) breaking, for which the wire stays in zone axis. In the case of SAC formation (Figure S4), the wire remained highly crystalline along the $\langle 111 \rangle$ direction, with a continuity of the dense plane across the junction. If twin planes are mobile, as previously reported,^{28,29} the apexes only rotates of few degrees ($\sim 2^\circ$) respectively to each other (Figure S4). SAC exhibit an important flexibility as evidenced by the drastic modification of its inclination, likely due to the mobility of the anchoring atoms.³⁰ The interatomic distance within atom chains was found in the range $0.23 - 0.31 \text{ nm}$, with a median at $0.29 \pm 0.10 \text{ nm}$, in agreement with the nearest-neighbor distance in gold (0.29 nm).³⁰ The larger interatomic distance of 0.31 nm , may result from the carbon contamination as previously reported.³¹ In the case of MAC (Figure S5), important recrystallization occurred. Contrarily to SAC, the dense planes are highly tilted, resulting in apex direction rotated of 23° respectively to the $\langle 111 \rangle$ direction. The position of atoms in the MAC, was analyzed and revealed unambiguously a portion of dense plane (60° angles) with slight positional disorder (Figure S5). The interatomic distance was found in the range $0.24 - 0.29$. Contrarily to the previous reports, the observed MAC is only one atom thick and do not exhibit helical multi-shell structure.³²

Concomitantly to the chain formation, individual Au atoms were steadily ejected and migrate from the shrinking channel. The trajectory of each atom could be followed, evidencing the formation of small clusters such as dimers or trimers. These clusters were fairly unstable and could dissociate after few seconds to yield isolated atoms. Such metallic clusters have been reported as highly reactive for catalysis, and in the case of gold, towards CO oxidation.^{33,34} Combined with the presence of the highly twinned and rough Au wires,³⁵ enhanced catalytic activities are expected.

Formation of quantized atomic channel along the wire length is clearly evidenced during the fragmentation process.

These intermediate states were stable enough to be imaged at 300 kV for few seconds. Modification of the wire surface energy, through ligands exchange process, could enable to further stabilize the single-atom thick chains,^{8,36} and thus open great perspective for the easy-made parallel quantized wires. Appearance of small and highly reactive clusters strengthens the potentiality of ultrathin Au nanowire for catalysis. Though studied under electron beam irradiation, similar breaking mechanism, involving channel shrinking and ejection of reactive atoms may occur under any external stimuli such as current flow or temperature rising, commonly used for Rayleigh instability studies.

ASSOCIATED CONTENT

Supporting Information

Experimental details and videos are available free of charge via the Internet at <http://pubs.acs.org>.

AUTHOR INFORMATION

Corresponding Author

Lise-Marie Lacroix. lmacroix@insa-toulouse.fr. Tel : +33567048833. Fax : +33561559697
Raul Arenal, arenal@unizar.es, Tel : +34976762985

Author Contributions

All the authors contributed equally.

Notes

The authors declare no competing financial interests.

ACKNOWLEDGMENT

The authors acknowledge the financial support of the Labex NEXT, N° 11 LABX 075, and of the European Associated Laboratory LEA TALEM. The scanning transmission electron microscopy studies were conducted at the Laboratorio de Microscopias Avanzadas (LMA) at the Instituto de Nanociencia de Aragón (INA) - Universidad de Zaragoza (Spain). The TEM measurements were supported by the European Union Seventh Framework Program under Grant Agreement 312483 - ESTEEM2 (Integrated Infrastructure Initiative - I3).

REFERENCES

- (1) Kisner, A.; Heggen, M.; Mayer, D.; Simon, U.; Offenhäuser, A.; Mourzina, Y. *Nanoscale* **2014**, *6*, 5146.
- (2) Pud, S.; Kisner, A.; Heggen, M.; Belaineh, D.; Temirov, R.; Simon, U.; Offenhäuser, A.; Mourzina, Y.; Vitusevich, S. *Small* **2013**, *9*, 846.
- (3) Loubat, A.; Escoffier, W.; Lacroix, L.-M.; Viau, G.; Tan, R.; Carrey, J.; Warot-Fonrose, B.; Raquet, B. *Nano Res.* **2013**, *6*, 644.
- (4) Lagos, M. J.; Sato, F.; Autreto, P. a. S.; Galvão, D. S.; Rodrigues, V.; Ugarte, D. *Nanotechnology* **2010**, *21*, 485702.
- (5) Olesen, L.; Laegsgaard, E.; Stensgaard, I.; Besenbacher, F.; Schiøtz, J.; Stoltze, P.; Jacobsen, K. W.; Nørskov, J. *K. Phys. Rev. Lett.* **1994**, *72*, 2251.
- (6) Ohnishi, H.; Kondo, Y.; Takayanagi, K. *Nature* **1998**, *395*, 780.
- (7) Yanson, A. I.; Bollinger, G. R.; Van den Brom, H. E.; Agrait, N.; Van Ruitenbeek, J. M. *Nature* **1998**, *395*, 783.
- (8) Leroux, Y. R.; Fave, C.; Zigah, D.; Trippé-Allard, G.; Lacroix, J. C. *J. Am. Chem. Soc.* **2008**, *130*, 13465.
- (9) Halder, A.; Ravishankar, N. *Adv. Mater.* **2007**, *19*, 1854.
- (10) Feng, H.; Yang, Y.; You, Y.; Li, G.; Guo, J.; Yu, T.; Shen, Z.; Wu, T.; Xing, B. *Chem. Commun.* **2009**, 1984.
- (11) Kang, Y.; Ye, X.; Murray, C. B. *Angew. Chem. Int. Ed.* **2010**, *49*, 6156.
- (12) Pazos-Pérez, N.; Baranov, D.; Irsen, S.; Hilgendorff, M.; Liz-Marzán, L. M.; Giersig, M. *Langmuir* **2008**, *24*, 9855.
- (13) Roy, A.; Pandey, T.; Ravishankar, N.; Singh, A. K. *AIP Adv.* **2013**, *3*, 032131.
- (14) Chandni, U.; Kundu, P.; Kundu, S.; Ravishankar, N.; Ghosh, A. *Adv. Mater.* **2013**, *25*, 2486.
- (15) Chandni, U.; Kundu, P.; Singh, A. K.; Ravishankar, N.; Ghosh, A. *ACS Nano* **2011**, *5*, 8398.
- (16) Karim, S.; Toimil-Molares, M. E.; Ensinger, W.; Balogh, A. G.; Cornelius, T. W.; Khan, E. U.; Neumann, R. *J. Phys. Appl. Phys.* **2007**, *40*, 3767.
- (17) Karim, S.; Toimil-Molares, M. E.; Balogh, A. G.; Ensinger, W.; Cornelius, T. W.; Khan, E. U.; Neumann, R. *Nanotechnology* **2006**, *17*, 5954.
- (18) Ciuculescu, D.; Dumestre, F.; Comesaña-Hermo, M.; Chaudret, B.; Spasova, M.; Farle, M.; Amiens, C. *Chem. Mater.* **2009**, *21*, 3987.
- (19) Kura, H.; Ogawa, T. *J. Appl. Phys.* **2010**, *107*, 074310.
- (20) Marks, L. D. *Rep. Prog. Phys.* **1994**, *57*, 603.
- (21) Arenal, R.; Lopez-Bezanilla, A. *ACS Nano* **2014**, *8*, 8419
- (22) *In-situ Electron Microscopy at High Resolution*; World Scientific, 2008.
- (23) Loubat, A.; Impéror-Clerc, M.; Pansu, B.; Meneau, F.; Raquet, B.; Viau, G.; Lacroix, L.-M. *Langmuir* **2014**, *30*, 4005.
- (24) Wang, Z. W.; Palmer, R. E. *Nanoscale* **2012**, *4*, 4947.
- (25) Smith, D. J.; Petford-Long, A. K.; Wallenberg, L. R.; Bovin, J.-O. *Science* **1986**, *233*, 872.
- (26) Nichols, F. A. *J. Mater. Sci.* **1976**, *11*, 1077.
- (27) Rodrigues, V.; Fuhrer, T.; Ugarte, D. *Phys. Rev. Lett.* **2000**, *85*, 4124.
- (28) Roy, A.; Kundu, S.; Müller, K.; Rosenauer, A.; Singh, S.; Pant, P.; Gururajan, M. P.; Kumar, P.; Weissmüller, J.; Singh, A. K.; Ravishankar, N. *Nano Lett.* **2014**, *14*, 4859.
- (29) Kundu, P.; Turner, S.; Van Aert, S.; Ravishankar, N.; Van Tendeloo, G. *ACS Nano* **2014**, *8*, 599.
- (30) Rodrigues, V.; Ugarte, D. *Phys. Rev. B* **2001**, *63*.
- (31) Galvão, D. S.; Rodrigues, V.; Ugarte, D.; Legoas, S. B. *Mater. Res.* **2004**, *7*, 339.
- (32) Kondo, Y. *Science* **2000**, *289*, 606.
- (33) Corma, A.; Concepción, P.; Boronat, M.; Sabater, M. J.; Navas, J.; Yacaman, M. J.; Larios, E.; Posadas, A.; López-Quintela, M. A.; Buceta, D.; Mendoza, E.; Guileira, G.; Mayoral, A. *Nat. Chem.* **2013**, *5*, 775.
- (34) Zhou, M.; Zhang, A.; Dai, Z.; Zhang, C.; Feng, Y. P. *J. Chem. Phys.* **2010**, *132*, 194704.
- (35) Rashkeev, S.; Lupini, A.; Overbury, S.; Pennycook, S.; Pantelides, S. *Phys. Rev. B* **2007**, *76*.
- (36) Huisman, E. H.; Trouwborst, M. L.; Bakker, F. L.; de Boer, B.; van Wees, B. J.; van der Molen, S. J. *Nano Lett.* **2008**, *8*, 3381.

Table of Content

